LEADING-EDGE RECEPTIVITY FOR BLUNT-NOSE BODIES

NASA Grant NAG-1-1135
Annual Progress Report
May 1, 1990 — April 30, 1991

Edward J. Kerschen
University of Arizona
Tucson, Arizona 85721

SUMMARY

This research program investigates boundary-layer receptivity in the leading-edge region for bodies with blunt leading edges. Receptivity theory provides the link between the unsteady disturbance environment in the free stream and the initial amplitudes of the instability waves in the boundary layer. This is a critical problem which must be addressed in order to develop more accurate prediction methods for boundary-layer transition. The first phase of this project examines the effects of leading-edge bluntness and aerodynamic loading for low Mach number flows. In the second phase of the project, the investigation will be extended to supersonic Mach numbers. Singular perturbation techniques are utilized to develop an asymptotic theory for high Reynolds numbers. In a parallel, closely coordinated effort, the author is collaborating with Dr. T.B. Gatski of NASA LaRC in utilizing his Navier-Stokes code for computations of leading-edge receptivity.

In this first year of the project, we have developed the asymptotic theory for leading-edge receptivity in low Mach number flows. The case of a parabolic nose is

considered, with $S = \omega r_n / U_\infty = O(1)$. The asymptotic theory for the unsteady flow utilizes the small parameter $\epsilon = (\omega\nu/U_\infty^2)^{1/6}$. In the outer region away from the body surface, an inviscid solution holds. The viscous analysis in the boundary layer involves two streamwise regions. In the region $\omega x/U_\infty = O(1)$, the disturbances satisfy the linearized, unsteady boundary-layer equation (LUBLE). Farther downstream where $\omega x/U_\infty = O(\epsilon^{-2})$, an asymptotic form of the Orr-Sommerfeld equation (OSE) applies. The inviscid solution in the outer region has been calculated, and the asymptotic eigenfunctions for the LUBLE have been derived and matched with the Tollmien-Schlichting (TS) wave of the OSE. This matching shows that the coefficient C_1 of the first asymptotic eigenfunction of the LUBLE determines the amplitude of the TS wave. To complete the asymptotic analysis, the coefficient C_1 of the asymptotic eigenfunction must be determined from a numerical solution of the LUBLE. We are presently addressing this task.

Substantial progress has also been made on the Navier-Stokes computations. Analytical solutions for the steady and unsteady potential flow fields have been incorporated into Dr. Gatski's code, greatly expanding the types of free-stream disturbances that can be considered while also significantly reducing the computational requirements. The time-stepping algorithm has been modified so that the potential flow perturbations induced by the unsteady pressure field are directly introduced throughout the computational domain, avoiding an artificial "numerical diffusion" of these from the outer boundary. In addition, the start-up process has been modified by introducing the transient Stokes wave solution into the downstream boundary condition. These modifications have significantly improved the performance of the code, and we anticipate that within a few months computational results will be available for comparison with the asymptotic theory. This will be the first comparison of asymptotic and Navier-Stokes results for leading-edge receptivity.

PROGRESS REPORT

The accurate prediction of boundary-layer transition and the need to control this phenomenon are becoming increasingly important in the development of advanced aeronautical vehicles. These requirements have focused renewed attention on the physics of the transition process. It was known for many years that boundary-layer transition is significantly influenced by the free-stream disturbance environment. However, the physical mechanisms by which energy is transferred from the long-wavelength, free-stream disturbances to the short-wavelength, instability waves were not understood. This came to be known as the receptivity problem.

Recent work by Goldstein and extensions by the author and his students have shown that the receptivity process takes place in regions of the boundary layer where the mean flow exhibits rapid changes in the streamwise direction. This occurs (*a*) near the body leading edge and (*b*) in any region farther downstream where some local feature forces the boundary layer to adjust on a short streamwise length scale. The rapid streamwise adjustment in these regions requires that nonparallel mean flow effects be included at leading order, in contrast to the parallel flow or slowly diverging flow assumptions utilized in stability theory. The current status of research in receptivity is summarized in several articles contained in Ref. 1.

Previous theoretical research in receptivity near leading edges has focused on the Blasius boundary layer on a semi-infinite, zero-thickness plate. The motion has been assumed to be incompressible and two-dimensional. Goldstein[2] utilized a high Reynolds number asymptotic approach to develop a theoretical framework for leading edge receptivity. The small parameter ϵ utilized in the analysis is defined by $\epsilon = (\omega\nu/U_\infty^2)^{1/6}$; note that ϵ^6 is the frequency parameter F for classical stability theory, which can also be interpreted as the inverse of a Reynolds number based on the convective wavelength U_∞/ω of the unsteady motion.

Two distinct streamwise regions arise in the asymptotic analysis. Near the leading edge where $\omega x/U_\infty = O(1)$, the unsteady motion is governed by the linearized unsteady boundary layer equation (LUBLE). In the second streamwise region farther downstream where $\omega x/U_\infty = O(\epsilon^{-2})$, the unsteady motion is governed by the classical large Reynolds number, small wavenumber approximation to the Orr-Sommerfeld equation (OSE). The Tollmien-Schlichting (TS) wave in the latter region corresponds to the triple deck structure of Smith[3]. Goldstein examined the asymptotic matching of these two regions, and showed that Lam and Rott's first asymptotic eigenfunction[4] for the LUBLE matches onto the TS wave of the OSE. Thus, the first asymptotic eigensolution of Lam and Rott is the precursor of the TS wave, and the coefficient C_1 of this asymptotic eigensolution determines the amplitude of the TS wave. Hence, we call C_1 the "Receptivity Coefficient."

The available results for the Receptivity Coefficient are restricted to the low Mach number, Blasius boundary layer on a semi-infinite, zero-thickness plate. The first calculation of a Receptivity Coefficient was presented by Goldstein, Sockol and Sanz[5] for the case of an acoustic wave propagating downstream parallel to the plate surface. The author and Heinrich[6,7] utilized information on the analytic structure of the solution to develop a much more accurate approach for calculation of the Receptivity Coefficient. Using this improved method, they calculated Receptivity Coefficients for a wide range of free-stream disturbances including obliquely incident acoustic waves, convected gusts (the linear representation of free-stream turbulence) of various orientations, and a von Karman vortex street passing above the plate surface. The Receptivity Coefficients for obliquely incident acoustic waves were found to be an order of magnitude larger than those for other free-stream disturbances. These large receptivity levels arise arise due to the strong diffraction field produced by the interaction of an oblique acoustic wave with the plate leading edge.

In order to obtain predictions of relevance to practical applications, it is essential that leading-edge bluntness be incorporated into the theory for leading edge receptivity. All bodies of practical interest have a finite leading-edge radius r_n, which enters the receptivity problem through the nondimensional parameter $S = \omega r_n / U_\infty$. This parameter is typically $O(1)$ or larger in aerodynamic applications, and it may even be large enough in laboratory experiments to cause significant deviations from the zero-thickness result. In the Receptivity Panel at the ICASE/LaRC Workshop on Instability and Transition (see Ref. 1), both the author and Morkovin identified leading-edge thickness as an important area for future research.

A second disadvantage of the zero-thickness geometry is that the influence of mean aerodynamic loading cannot be investigated, since any asymmetrical mean flow component in the vicinity of the leading edge leads to boundary layer separation. It is well known that aerodynamic loading significantly influences both the mean boundary layer development and the stability of the boundary layer. Hence, it is reasonable to anticipate that aerodynamic loading is an important parameter in the receptivity problem as well. In fact, in his laboratory experiments Leehey[8] found that small changes in the "angle of attack" of his plate produced dramatic changes in the receptivity to acoustic waves. Thus, in order to obtain results which are relevant to practical applications, it is essential to incorporate both leading-edge bluntness and aerodynamic loading in the receptivity theory.

The present research program extends the asymptotic theory for leading edge receptivity to incorporate the effects of leading-edge bluntness, aerodynamic loading and compressibility. In the first phase of the program, the effects of leading-edge bluntness and aerodynamic loading are being investigated for the low Mach number case. In the second phase of the program, the theory will be extended to high Mach number flows. The low speed problem is viewed as an essential stepping stone in the development of the theory, and also has relevance to the high Mach number case

where a strong shock produces low speed flow near the nose of the body.

As an integral part of this research program, we are also collaborating with Dr. T.B. Gatski of NASA LaRC in Navier-Stokes computations for leading-edge receptivity. These computations are an important complement to the asymptotic theory, which provides valuable information regarding the dominant physical mechanisms and relevant scaling parameters, but may not provide sufficient quantitative accuracy for parameter ranges of practical interest. In particular, the Navier-Stokes computations allow finite Reynolds number effects to be assessed. The computations can also be utilized to investigate nonlinear effects due to free-stream disturbances of finite amplitude.

For the low Mach number study which forms the first phase of this research project, we consider conventional airfoil shapes which have a parabolic leading edge. The streamwise length scale for the leading-edge receptivity analysis is the convected wavelength U_∞/ω, which is generally small compared to the airfoil chord b. Hence, it is only the airfoil characteristics near the leading edge which enter the analysis, and the geometry can be restricted to a semi-infinite parabola with the nose radius r_n of the airfoil. For a symmetric airfoil at zero angle of attack, the flow past the leading edge is symmetric. However, aerodynamic loading due to camber or a nonzero angle of attack produces a flow asymmetry. In the local leading-edge region, this asymmetry corresponds to a flow component around the leading edge from the pressure side to the suction side. The application of the method of Matched Asymptotic Expansions[9] for a nose radius r_n small compared to the airfoil chord b shows that, in the local leading-edge region, the complex potential for the inviscid mean flow has the asymptotic expansion

$$W(z) = \Phi + i\Psi = U_\infty \left[\sqrt{z} - i\sqrt{r_n/2}\right]^2 + U_\infty \alpha_{eff} b^{1/2} \left[\sqrt{z} - i\sqrt{r_n/2}\right] + \ldots \quad (1)$$

where $z = x + iy$. The first term corresponds to the symmetric component of the local flow past the leading edge, while the second term is the asymmetrical component produced by the airfoil camber and angle of attack. An expression for α_{eff} in terms of the airfoil angle of attack and camber distribution is given in Ref. 10. In our work to date, we have concentrated on the case of leading-edge bluntness for a symmetric mean flow ($\alpha_{eff} = 0$). The extension to include nonzero values of α_{eff} is conceptually straightforward and will be carried out later. Details of our progress on the Navier-Stokes computations and on the asymptotic theory are discussed separately below.

Navier-Stokes Computations

In the first few months of the project, we focused on the collaboration with Dr. Gatski in Navier-Stokes computations for leading-edge receptivity. Dr. Gatski's code[11] is well suited to the study of leading-edge receptivity, since it solves the Navier-Stokes equations in parabolic coordinates. Hence, no discontinuities in the geometry, grid generation functions, or related derivatives are present in the numerical approach. Receptivity is a sensitive phenomenon and such discontinuities could easily lead to spurious "numerical sources" of receptivity.

The Navier-Stokes computation of the unsteady flow past a parabola is a difficult problem on which previous investigators have had only partial success. Murdock attempted an incompressible, Navier-Stokes calculation of receptivity at the leading edge of a parabola, and presented a preliminary report in a conference paper[12]. However, Murdock never published this work in archival form because his downstream boundary condition caused difficulties which he never satisfactorily resolved (private communication, June 1990). Reed *et al*[13] have presented incompressible computations for geometries consisting of an elliptical nose attached to a flat plate. Unfortunately, her results appear to be dominated by localized receptivity[14] at the

junction between the elliptical nose and the flat plate, and may also be contaminated by "spurious sources" related to the numerical treatment of the abrupt discontinuity in curvature at the junction between the elliptical nose and the flat plate.

Both Murdock and Reed introduced the flow unsteadiness by specifying a uniform axial pulsation on the outer boundary of the computational domain far from the body surface. This boundary condition is an attempt to model receptivity to a parallel, plane acoustic wave in the limit $M \rightarrow 0$. However, the author's previous asymptotic studies have shown that it is oblique acoustic waves which are primarily responsible for leading-edge receptivity at low Mach numbers. The approaches of Murdock and Reed are not easily modified to treat the case of obliquely incident acoustic waves. In addition, even for the parallel plane wave case, the actual unsteady flow far from the body consists of the superposition of an incident, plane acoustic wave and a scattered, outgoing, cylindrical acoustic wave. Since the amplitude of the scattered wave decays only as the square root of distance from the body nose, the assumption of a uniform axial pulsation at a finite distance from the body is questionable.

Our computational approach takes advantage of singular perturbation concepts and has several advantages compared to the approaches utilized by Murdock and Reed. In contrast to these authors, we utilize analytical solutions for the steady and unsteady components of the potential flow outside the boundary layer. The singular perturbation approach allows us to correctly account for the scattering of the incident acoustic wave by the body surface, and to treat the important case of obliquely incident acoustic waves. Furthermore, with our singular perturbation approach these features can be captured without considering flow compressibility in the Navier-Stokes computation. This is discussed in more detail in the following section. Finally, in contrast to the approaches of Murdock and Reed, our computational domain can be restricted to the viscous portion of the flow field. This significantly decreases the

computational effort and provides advantages relative to the accuracy and resolution of the results.

Two additional modifications which we have introduced into the Navier-Stokes code also merit discussion. The code is a velocity-vorticity formulation. The convection and diffusion of the vorticity field is calculated in the first half of the time step. In the second half of the time step, an iterative solver is applied to the divergence and curl relations in order to update the velocity field. In our early unsteady flow calculations, we experienced difficulties due to a gradual buildup of numerical errors related to incomplete relaxation in the iterative solver. This difficulty could be suppressed by significantly reducing the time step, but this resulted in prohibitive computation times.

After some study, we realized that this difficulty was due to the way in which time variations in the potential flow field were being introduced into the code. The change in the inviscid slip velocity was being introduced through the outer boundary condition in the second half of the time step, and in each iteration of the velocity solver the adjustment in the potential flow field "diffused" inward only one grid level. Thus, a large number of iterations were required to "numerically diffuse" the change in the potential flow field. This characteristic of the numerical algorithm was inconsistent with the inherent physics of the problem, since adjustments to a potential flow are instantaneously transmitted throughout the field via the unsteady pressure distribution.

To more accurately model the physics of the problem, we modified the numerical algorithm such that the change in the potential flow field was introduced throughout the computational domain prior to applying the iterative solver in the second half of the time step. This modification dramatically improved the behavior of the algorithm. Much larger time steps can now be used with no indications of numerical difficulties.

After incorporating this change in the code, calculations were carried out over time intervals corresponding to several periods of the unsteady motion. The results obtained were in general very encouraging, but contained one feature which we view with some skepticism. Instability waves appear to be originating near the downstream boundary of the computational domain. It is possible that these instability waves are being generated by Morkovin's mechanism of unsteady free-stream pressure gradients, which could arise due to the interaction of free-stream acoustic waves with the curvature of the surface. To investigate this possibility, we are currently performing calculations for the flat plate case, in which Morkovin's mechanism would not be operative. However, in recent work[15] we have shown that the instability waves produced by Morkovin's mechanism have exponentially small amplitudes whenever the length scale of the free-stream pressure gradient is long compared to the instability wavelength. Hence, it seems likely that another mechanism is producing these waves. In our previous computations, we found that the solutions are fairly sensitive to the downstream boundary condition. Thus, we are also exploring the possibility that these waves could be spuriously generated by the downstream boundary condition.

The asymptotic theory for leading-edge receptivity shows that the TS waves are generated near the leading edge where $\omega x/U_\infty = O(1)$. Hence, in a transient problem in which the unsteady motion is initiated at $t = 0$, TS wave motion should appear first in the upstream region. This TS wave motion should then gradually move downstream as the unsteady flow field evolves. Thus, in the early stages of the unsteady flow development, the unsteady motion at the downstream boundary should simply consist of the Stokes wave induced by the local unsteady potential flow.

In the computations described above, the time-harmonic motion $\sin\omega t$ was "switched on" at $t = 0$. However, we utilized the "steady-state" time-harmonic Stokes wave solution in the downstream boundary condition. The "switch on" of the time-harmonic Stokes problem has been investigated by Panton[16], who found that the tran-

sient died off in less than one period of the motion. However, we are concerned that the initial inconsistency in the outflow boundary condition may produce a spurious "numerical source" of receptivity. To investigate this issue, we are presently incorporating the transient Stokes solution into our downstream boundary condition.

The computational work described in this section is being closely coordinated with the development of the asymptotic theory, which is described in the following section.

Asymptotic Theory

We now discuss our progress on the asymptotic theory for leading-edge receptivity. The asymptotic analysis requires a sophisticated understanding of applied mathematics and fluid dynamics. Thus, in order to make timely progress on this project, a Post Doctoral student is required. Paul Hammerton was selected from a number of candidates for this Post Doctoral position. Hammerton received his Ph.D. in 1990 from the University of Cambridge. His dissertation advisor was David Crighton in the Department of Applied Mathematics and Theoretical Physics. Hammerton accepted a two-year appointment at the University of Arizona, and arrived at Arizona in early November. He is taking primary responsibility for carrying out the detailed asymptotic analysis of the viscous motion, and has rapidly come up to speed on the subject of boundary-layer receptivity.

Both the asymptotic theory and the Navier-Stokes computations rely on analytical solutions for the steady and unsteady components of the potential flow field. Thus, this part of the analysis was developed by the author prior to Hammerton's arrival in Arizona. The steady component of the potential flow field corresponds to inviscid flow past a parabola and is well known. The unsteady component of the potential flow field corresponds to scattering of a plane acoustic wave by a semi-

infinite parabola in a low Mach number flow. We have analyzed this problem using singular perturbation techniques.

It might at first appear that the acoustic scattering problem in the limit $M \to 0$ could be analyzed simply by assuming that the flow is incompressible. However, the author and Heinrich[6] showed that acoustic scattering problems involving semi-infinite bodies are singular in the limit $M \to 0$. Thus, the local flow field in the vicinity of the leading edge cannot be calculated without also considering a global region in which the acoustic wavelength λ is the appropriate length scale. For the semi-infinite parabola with $S = \omega r_n / U_\infty = O(1)$ and $M = U_\infty / c << 1$, the parabola appears to be very thin when viewed on the scale of the acoustic wavelength $\lambda = 2\pi c/\omega$. Thus, the leading order term of the global solution is the classical problem of diffraction by a semi-infinite, zero-thickness plate. We utilize the Wiener-Hopf technique[17] to obtain the leading term of the global solution in the form

$$\phi_0(x,y) = \frac{p_{ac}}{\rho c}\left\{-\frac{i}{k}e^{ik(x\cos\theta_{ac} - y\sin\theta_{ac})} + \sin\frac{\theta_{ac}}{2}\,\frac{sgn(y)}{\pi\sqrt{2k}}\int_{-\infty}^{\infty}\frac{\exp(-\sqrt{\lambda^2 - k^2}\,|y| - i\lambda x)}{(\lambda + k\cos\theta_{ac})\sqrt{\lambda + k}}\,d\lambda\right\}e^{-i\omega t} . \quad (2a)$$

Here (x,y) are dimensional coordinates centered at the focus of the parabola, $p_{ac}/\rho c$ is the magnitude of the velocity fluctuation associated with the incident acoustic wave, θ_{ac} is the incidence angle of the acoustic wave measured with respect to the body axis, and $k = \omega/c$ is the acoustic wavenumber. For matching with the local region near the leading edge, the asymptotic expansion of this solution as $r = \sqrt{x^2 + y^2} \to 0$ is required. From Fourier transform theory, it is known that the behavior of the integral in (2*a*) for small (x,y) is related to the behavior of the transform function for large λ. Thus, we find that the small argument expansion of $\phi_0(x,y)$ takes the form

$$\phi_0(x,y) \sim \frac{p_{ac}}{\rho c}\left[-\frac{i}{k} - 2^{3/2}\frac{e^{i\pi/4}}{\sqrt{\pi k}}\sin\frac{\theta_{ac}}{2}\sqrt{r}\cos\frac{\theta}{2} + \cos\theta_{ac}\, r\cos\theta + O(r^{3/2})\right] e^{-i\omega t} \qquad (2b)$$

where (r,θ) is the polar form of (x,y).

In the local leading-edge region, the appropriate length scale is the nose radius r_n. The asymptotic analysis of the viscous motion utilizes coordinates nondimensionalized on the length scale U_∞/ω, with the nondimensional nose radius $S = \omega r_n/U_\infty$ assumed to be $O(1)$. Hence, anticipating the viscous analysis, it is convenient to also express the potential flow solution in the local leading-edge region in terms of coordinates nondimensionalized by U_∞/ω. Since $r_n << \lambda$, the unsteady component of the potential flow in the local leading-edge region is incompressible and consists of a sum of eigensolutions

$$\Phi_0(x,y) = \frac{p_{ac}}{\rho c}\frac{U_\infty}{\omega}\left(A + B\,\mathrm{Re}\left[\sqrt{Z} - i\sqrt{S/2}\right] + C\,\mathrm{Re}\left[\left[\sqrt{Z} - i\sqrt{S/2}\right]^2\right] + \ldots\right)e^{-i\omega t} \qquad (3a)$$

where $Z = \omega(x + iy)/U_\infty$ and A, B and C are undetermined coefficients. Expanding $(3a)$ for large Z and matching with $(2b)$, the constants are determined as

$$A = -\frac{i}{M}, \quad B = -\frac{2^{3/2}e^{i\pi/4}}{\sqrt{\pi}}\frac{\sin\theta_{ac}/2}{\sqrt{M}} \quad \text{and} \quad C = \cos\theta_{ac}\,. \qquad (3b)$$

Physically, the function whose coefficient is B corresponds to an asymmetric, unsteady potential flow around the nose of the parabola, while the function whose coefficient is C corresponds to a symmetric, unsteady potential flow. For the case of an incident plane wave parallel to the axis of the parabola ($\theta_{ac} = 0^o$), the coefficient B vanishes and C is $O(1)$. This is the case modeled in the computations of Murdock and Reed. In contrast, for the case of an obliquely incident acoustic wave, $B = O(M^{-1/2})$. Thus, at low Mach numbers, an oblique acoustic wave generates a strong asymmetric flow around the leading edge. This asymmetric flow in turn produces a strong

unsteady response in the boundary layer, leading to high values of leading-edge receptivity. Equations (3) provide the outer boundary conditions for both our Navier-Stokes computations and our asymptotic analysis of leading-edge receptivity.

We now turn to the asymptotic analysis of the viscous motion in the boundary layer. As discussed above, the analysis of the viscous motion involves two distinct streamwise regions, the LUBLE region near the leading edge in which $\omega x/U_\infty = O(1)$, and the OSE region farther downstream in which $\omega x/U_\infty = O(\epsilon^{-2})$, where $\epsilon = (\omega\nu/U_\infty{}^2)^{1/6}$ is the small parameter in the asymptotic analysis. The asymptotic structure of the unsteady viscous motion is illustrated in Figure 1.

The viscous analysis is most conveniently developed in a parabolic coordinates, defined by

$$x = \frac{U_\infty}{\omega}\,\frac{1}{2}\,(\xi^2 - \eta^2) \qquad \text{and} \qquad y = \frac{U_\infty}{\omega}\,\xi\eta\,, \tag{4a,b}$$

where x and y are Cartesian coordinates in the streamwise and cross-stream directions, respectively. We have nondimensionalized the physical coordinates (x,y) by U_∞/ω, so that the LUBLE region corresponds to $\xi = O(1)$ and the body surface is given by $\eta = S^{1/2}$. To thoroughly investigate the effect of nose bluntness, the analysis is developed for the case $S = O(1)$. The viscous motion in the boundary layer is driven by the unsteady slip velocity associated with (3). Expressing (3) in parabolic coordinates and setting $\eta = S^{1/2}$, the unsteady slip velocity is given by

$$u_{sl} = \frac{p_{ac}}{\rho c}\left\{ -\frac{2\,e^{i\pi/4}}{\sqrt{\pi M}}\sin\frac{\theta_{ac}}{2}\,\frac{1}{\sqrt{\xi^2+S}} + \cos\theta_{ac}\,\frac{\xi}{\sqrt{\xi^2+S}}\right\}e^{-i\omega t}\,. \tag{5}$$

It can be seen from this expression that the nose radius of the parabola limits the peak velocity associated with the strong asymmetric flow due to obliquely incident acoustic waves.

Since the thickness of the mean boundary layer is of the order of the square root of the Reynolds number, we introduce a boundary layer coordinate η where

$$\eta = S^{1/2} + \epsilon^3 \eta \,. \qquad (6a,b)$$

Separating the streamfunction into a steady flow component $\Psi(\xi,\eta)$ and an unsteady disturbance $\psi(\xi,\eta)e^{-i\omega t}$, and linearizing the equation for ψ, the unsteady flow in the boundary layer is found to satisfy the linearized unsteady boundary layer equation (LUBLE)

$$\psi_{\eta\eta\eta} + \Psi_{\eta\eta}\,\psi_\xi + \Psi_\xi\,\psi_{\eta\eta} - \Psi_\eta\,\psi_{\xi\eta} - \Psi_{\xi\eta}\,\psi_\nu + \frac{2\xi}{H^2}\,\Psi_\eta\,\psi_\eta + iH^2\,\psi_\eta = H^3\left[\, i - \frac{S}{H^4} - \frac{\xi}{H^2}\,\frac{\partial}{\partial\xi}\,\right] u_{sl}(\xi) \qquad (7)$$

where $H^2 = \xi^2 + S$ arises from the Jacobian of the transformation from Cartesian to parabolic coordinates. The right hand side of this equation is the unsteady pressure gradient impressed on the boundary layer by the unsteady potential flow. At $\eta = 0$, ψ and ψ_η are zero, and ψ_η must match with the inviscid slip velocity as $\eta \to \infty$.

For $\xi = O(1)$, solutions for Ψ and ψ can be found only by using numerical methods, which we shall discuss in due course. However, for large values of ξ well downstream of the nose, an asymptotic solution for (7) can be derived. This asymptotic solution consists of a Stokes wave which is related to the inviscid forcing field, plus an infinite set of asymptotic eigensolutions. The first asymptotic eigensolution is the precursor of the TS wave, and thus is of fundamental importance in the theory of leading edge receptivity.

In calculating the asymptotic eigensolutions of (7), we utilize Van Dyke's[18] result for the mean boundary layer far downstream on the surface of a parabola in a uniform stream. He found that the streamfunction for the mean flow has the expansion

$$\Psi = \xi \left[F(\eta) + \frac{S}{\xi^2} \log (\xi^2/S)\, A_1 \left[\eta F' - F\right] + \frac{S}{\xi^2}\left[B_1 \left[\eta F' - F\right] + f(\eta)\right] + \ldots \right] \quad (8)$$

where A_1 and B_1 are numerical constants, F is the Blasius function and f satisfies a prescribed ordinary differential equation. This expansion shows that, far downstream, the boundary layer on a parabola approaches that for a flat plate. Physically, the term involving B_1 represents a slight shift in the effective origin for this flat plate.

Utilizing (8) for the mean flow description, we develop an asymptotic solution of the LUBLE (7) for $\xi >> 1$. The most important feature of this solution is the first asymptotic eigensolution. The asymptotic eigensolution has a two-layer structure in the direction normal to the surface. The inner layer corresponds to $\eta = O(\xi^{-1})$, while the the outer layer has the same thickness as the mean boundary layer, $\eta = O(1)$. In analyzing the inner layer, it proves convenient to introduce a modified transverse coordinate $m = \xi\eta(1 + S/2\xi^2)$. The use of this coordinate simplifies the solution by taking partial account of the parabolic geometry. In the inner layer, the expression for the first asymptotic eigensolution has the form

$$\psi = C_1(S)\, \xi^{2\tau}\, e^{-T(\xi)} \left[p_0(m) + \xi^{-3}\, p_1(m) + \ldots \right] \quad (9a)$$

where

$$T(\xi) = \frac{\lambda\,(1-i)\,\xi^3}{3\,U_0'} \left\{ 1 + 3A_1\, \frac{S}{\xi^2} \ln (S/\xi^2) + 3 \left[\frac{3}{2} - B_1 + 2A_1 \right] \frac{S}{\xi^2} \right\} \quad (9b)$$

and U_0' denotes $U'(0)$. Equation (9) generalizes Lam and Rott's[4] asymptotic eigensolution for the flat plate to the case of a parabolic cylinder. The constant λ in (9*b*) is a (real) eigenvalue entering the governing equation for $p_0(m)$. The leading edge bluntness has produced logarithmic terms in the exponent $T(\xi)$. The value of τ, a numerical constant, is fixed by the solvability condition for $p_1(m)$, the second term in (9*a*). This gives

$$\tau = \tau_{S=0} + \frac{S\,\lambda}{2\,U_0'^2}\left\{1 - \frac{1}{2}\,\frac{\left[\int_0^\infty w\,dm\right]^2}{\int_0^\infty m\,w^2\,dm}\right\} \qquad (10a)$$

where $\tau_{S=0}$ is the value for the flat plate case and $w(m) = p_0''(m)$ is expressible in terms of an Airy function. Thus, in the exponent τ, the leading edge bluntness produces an order-one change to the flat plate result. Goldstein[5] calculated the flat-plate value $\tau_{S=0} \simeq -0.69$. Evaluating (10*a*), τ has the complex value

$$\tau \simeq -0.69 - S\,0.51\,(1 - i) \qquad (10b)$$

for the case of a parabolic leading edge. The imaginary part of τ is allied to the appearance of logarithmic terms in $T(\xi)$. Physically, the imaginary component of τ is equivalent to a logarithmic term in the phase of the asymptotic eigensolution.

The coefficient C_1 multiplying the asymptotic eigensolution in (9) is arbitrary within the asymptotic analysis, and hence must be found from a numerical solution of the LUBLE. This is discussed below. In general, C_1 is a function of the nondimensional nose radius S and of the specific free-stream disturbance.

The coordinate transformation (4*a*) shows that distance downstream is proportional to ξ^2. Hence, the cubic term in (9*b*) implies that the wavelength of the asymptotic eigensolution is proportional to $x^{-1/2}$. As the wavelength decreases with distance downstream, the pressure fluctuations induced by the unsteady displacement thickness of the asymptotic eigensolution increase in importance. When $\xi = O(\epsilon^{-1})$, this self-induced pressure gradient exerts an order-one influence on the unsteady motion. Since the two-layer solution (9) ignores this pressure field, it becomes invalid in this region. Therefore, the two-layer solution must be replaced by a new asymptotic solution. This new solution turns out to be the high Reynolds number, small wavenumber asymptotic expansion for the Orr-Sommerfeld equation (OSE). This asymptotic expansion corresponds to a triple-deck structure, in which the two layers of the

previous solution are supplemented by a third layer just outside the mean boundary layer. This third layer is the potential flow which enters the interactive pressure-displacement relation.

Anticipating the asymptotic matching of the LUBLE and OSE regions, the TS wave in the OSE region has the expansion

$$\psi = \epsilon^{-2\tau} A(\xi_1)\, \gamma(\eta,\epsilon) \exp\left[\frac{i}{\epsilon^3} \int^{\xi_1} \xi_1' \kappa(\xi_1',\epsilon)\, d\xi_1' \right] \tag{11}$$

where $\xi_1 = \epsilon\xi = O(1)$, τ is given by (10), $A(\xi_1)$ is a slowly varying amplitude, γ is the mode shape and κ is the complex wavenumber. With suitable changes in the definition of the wavenumber α, phase speed c and Reynolds number R, the OSE for the parabolic geometry can be reduced to the standard form for the flat plate. Specifically, we set

$$\alpha = \alpha_{S=0}\left[1 + S\,\frac{\epsilon^2}{\xi_1^2} \right], \quad c = c_{S=0}\left[1 + S\,\frac{\epsilon^2}{2\xi_1^2} \right],$$

and

$$\alpha R = (\alpha R)_{S=0}\left[1 + S\,\frac{\epsilon^2}{\xi_1^2} \right]. \tag{12a,b,c}$$

Here the subscript S=0 refers to the appropriate values for the flat plate case.

At first sight these corrections would appear to have little effect on the form of the TS wave structure, beyond modifying the slow spatial variation of the wave amplitude. However, a careful analysis of the modified equation demonstrates that the standard results of the triple-deck theory for the flat plate case are not directly applicable. The mean flow pressure gradient leads to a crucial difference in the boundary layer profile close to the body surface, namely $U''(0) \neq 0$. Thus the complex wavenumber obtained by Goldstein[2] for TS waves on a flat plate can not be readily modified to the parabolic geometry. However using similar methods, we have

obtained the following expansion of the wavenumber for the parabolic cylinder,

$$\kappa(\xi_1) = \left[\kappa_0 + \epsilon\,\kappa_1 + \epsilon^2\,\kappa_2\right] + S\left[\epsilon^2 \ln\epsilon\,\hat{\kappa}_{L,2} + \epsilon^2\,\hat{\kappa}_2\right] + O(\epsilon^3 \ln\epsilon)\,, \qquad (13a)$$

with the $\epsilon^2 \ln \epsilon$ term arising due to the first perturbation term in (9*b*). The functions κ_0, κ_1 and κ_2 are the flat plate values given by Goldstein[2]. The first two terms generated by the parabolic geometry are given by

$$\hat{\kappa}_{L,2} = \frac{e^{-i5\pi/4}}{Y^{3/2}}\,\frac{2A_1}{U_0'^2}\,\frac{1}{\tilde{\xi}_1}\left[1 - \frac{9}{2}\,\frac{\tilde{\xi}_1^3}{YH'(Y)}\right] \qquad (13b)$$

and

$$\hat{\kappa}_2 = -\frac{e^{-i5\pi/4}}{Y^{3/2}}\,\frac{1}{U'^2}\,\frac{1}{\tilde{\xi}_1}\left\{\left[B_1 + A_1 \ln(\xi_1^2/S)\right]\left[1 - \frac{9}{2}\,\frac{\tilde{\xi}_1^3}{YH'(Y)}\right] + \frac{3}{2}\left[1 - \frac{4\,\tilde{\xi}_1^3}{YH'(Y)}\right]\right\} \qquad (13c)$$

where

$$H(z) = \frac{e^{i5\pi/2}\,z^2\,Ai'(z)}{\int_\infty^z Ai(z')\,dz'}\,. \qquad (13d)$$

In these expressions, Y is defined by $H(Y) = \tilde{\xi}_1^3$ where $\tilde{\xi}_1 = \xi_1/U_0'$ and A_1 and B_1 are the numerical constants appearing in (8). It is interesting to note that the $O(\epsilon^2 \ln \epsilon)$ correction due to the parabolic geometry precedes the first correction due to nonparallel flow effects which is $O(\epsilon^3)$ in Smith's[3] flat plate theory.

The higher order terms for κ have also been determined, up to the ϵ^3 term which also determines the slowly varying amplitude function $A(\xi_1)$. This solution in the triple-layer region has been rigorously matched back to the asymptotic expansion (9*a*) for the LUBLE. This matching shows that the coefficient C_1 in (9*a*) determines the amplitude of the TS wave, and hence is the "Receptivity Coefficient." The further development of the TS wave with distance downstream over the parabolic cylinder, as described in (13), is not central to understanding the actual receptivity process.

However, the detailed effect of the parabolic geometry on the TS wave must be fully determined in order to allow comparison with the ongoing numerical investigation of Dr. Gatski.

As an illustration of these effects, Figures 2 and 3 show preliminary comparisons between the TS wavenumbers for a parabolic cylinder with $S = 1$ and for a flat plate, with $\epsilon = 0.1$ in both cases. The normalized coordinate $\tilde{\xi}_1$ has absorbed some of the effects of the parabolic geometry, and hence the neutral stability points for the two cases in Figure 3 are not markedly different. However, the favorable pressure gradient over the parabolic cylinder modifies both the wavelength and the growth rate of the instability wave. The favorable pressure gradient decreases $\mathrm{Re}(\kappa)$, corresponding to an increase in the TS wavelength (Figure 2), and further stabilizes the boundary layer, as is evident from the growth rates plotted in Figure 3.

At small ξ_1, the asymptotic results plotted in these figures become invalid as the region governed by the LUBLE (7) is approached and geometric effects become dominant. The lower limit $\tilde{\xi}_1^2 = 0.1$ corresponds to $\xi \simeq 1.6$ which is well within the region of significant wall curvature.

To determine the Receptivity Coefficient C_1, a numerical solution of the LUBLE for the particular free-stream disturbance of interest is required. Essentially, the numerical solution of the LUBLE for $\xi >> 1$ is compared with the expression (9*a*) for the first asymptotic eigensolution. We are now beginning to address this task, and are considering the merits of various numerical schemes. An important aspect of our approach is to utilize our knowledge of the analytical structure of the large ξ behavior. A critical feature of the problem is that for real ω and ξ, the first asymptotic eigensolution makes only an exponentially small contribution at large ξ. Thus, for real ξ, it would be extremely difficult to determine C_1 from a direct comparison of the numerical and asymptotic results. However, the LUBLE is analytic in ξ, and hence we extend the problem into the complex ξ plane and calculate the numerical solution

along a ray where the first asymptotic eigensolution is dominant. As in previous work by the author, we shall analytically factor out the now rapidly growing exponential factor $e^{-T(\xi)}$ of the first asymptotic eigensolution before discretizing the problem.

We anticipate that the development of a computer program to solve the LUBLE and extract the receptivity coefficient will take only a few months. By the time of the ICASE/LaRC workshop this summer, we should be well along in a parametric study based on our asymptotic theory. During the workshop we plan to make extensive comparisons of our asymptotic results with the numerical results generated by Dr. Gatski's Navier-Stokes code.

Concluding Remarks

In the first year of this research program, significant progress has been made on both the asymptotic theory and the collaborative Navier-Stokes computations of leading-edge receptivity. This project complements the NASA LaRC in-house activity on boundary-layer receptivity, which is focused mainly on localized rather than leading-edge mechanisms and involves the author's *ex*-student, Dr. M. Choudhari. We have developed a strong, mutually beneficial collaboration with Dr. Gatski in Navier-Stokes computations, and foresee additional opportunities for collaboration with other NASA computational fluid dynamicists. In particular, the author and Dr. C. Streett recently discussed possible interactions on spectral calculations of leading-edge receptivity, and we plan to explore this further during the ICASE/LaRC workshop this summer. Additional opportunities for collaborative activity would arise in the second phase of this research program, which extends the investigation to supersonic Mach numbers.

This project involves subtle physical mechanisms and sophisticated mathematical techniques, as can be seen from the above discussion of our progress on the

asymptotic theory. The significant background work in this area has been performed by outstanding senior researchers such as M.E. Goldstein and F.T. Smith. Thus, when the author proposed this project, he emphasized the importance of utilizing a Post Doctoral student. It would be quite difficult for a beginning graduate student to work through the relevant background literature, and even harder for him to understand how these analyses could be significantly extended. Indeed, if this project was attempted with a beginning Ph.D. student, the author would anticipate very little progress for at least a couple of years. The low Mach number study alone would be appropriate for a three (or four!) year Ph.D. project.

The argument is sometimes advanced that projects involving graduate students are preferable due to their educational component. Post Doctoral studies also have a strong educational component and in fact are becoming increasingly important for individuals seeking an academic position at a first-rate university. The education provided by Post Doctoral study is equally valuable for future positions in government or private research laboratories. An alternative viewpoint is that the choice of a Master's, Ph.D. or Post Doctoral student should be based on the difficulty of the project. In all three cases, the project contributes to the education of the student and to his future career development.

In summary, at this time our research on leading-edge receptivity is definitely on schedule, and possibly ahead of schedule. The asymptotic theory for the case of a symmetric, low Mach number mean flow is nearly complete. The only remaining task is the development of a computer program to solve the LUBLE and extract the receptivity coefficient C_1. The computer programming should take only a couple of months. During the ICASE/LaRC workshop this summer, we shall utilize the asymptotic theory to perform a parametric study of the influence of nose bluntness on leading-edge receptivity for low Mach number flows. Extensive comparisons of the asymptotic results and Dr. Gatski's Navier-Stokes simulations will also be carried out during the workshop.

REFERENCES

1. Hussaini, M.Y. and Voigt, R.G. (eds.) 1990. *Instability and Transition*, Vol 1, Proceedings of ICASE/LaRC Workshop on Stability and Transition, Springer-Verlag, New York.

2. Goldstein, M. E. 1983. The evolution of Tollmien-Schlichting waves near a leading edge. *J. Fluid Mech.* 127, 59-81.

3. Smith, F. T. 1979. On the non-parallel flow stability of the Blasius boundary layer. *Proc. Roy. Soc. London A* **366**, 91-109.

4. Lam, S. H. and Rott, N. 1960. Theory of linearized time-dependent boundary layers. *Cornell Univ. Grad. School of Aero. Engineering Rep. AFOSR TN-60-1100.*

5. Goldstein, M. E., Sockol, P. M., and Sanz, J. 1983. The evolution of Tollmien-Schlichting waves near a leading edge. Part 2. Numerical determination of amplitudes. *J. Fluid Mech.* 129, 443-453.

6. Heinrich, R. A. E. 1989. Flat plate leading edge receptivity to various free-stream disturbance structures. Ph.D. thesis, University of Arizona. (Archival papers under preparation.)

7. Heinrich, R. A. E. and Kerschen, E. J. 1989. Leading edge boundary layer receptivity to various free-stream disturbance structures. *Z. angew. Math. Mech.* **69** T596-T598.

8. Leehey, P. 1989. Private communication.

9. Van Dyke, M. D. 1975. *Perturbation Methods in Fluid Mechanics*, Parabolic Press, Stanford.

10. Myers, M. R. and Kerschen, E. J. 1986. Influence of airfoil camber on convected gust interaction noise. *AIAA 86-1873.*

11. Gatski, T. B., Grosch, C. E. and Rose, M. E. 1982. A numerical study of the two-dimensional Navier-Stokes equations in vorticity-velocity variables. *J. Comp. Phy.* **48**, 1-22.

12. Murdock, J.W. 1981. Tollmien-Schlichting waves generated by unsteady flow over parabolic cylinders. AIAA 81-0199.

13. Reed, H.L., Lin, N. and Saric, W.S. 1990. Boundary layer receptivity to sound: Navier-Stokes computations. *Appl. Mech. Rev.* **43**.

14. Goldstein, M. E. 1985. Scattering of acoustic waves into Tollmien-Schlichting waves by small streamwise variations in surface geometry. *J. Fluid Mech.* **54**, 509-529.

15. Heinrich, R. A. E., Gatski, T. B., and Kerschen, E. J. 1990. Boundary layer receptivity to unsteady free-stream pressure gradients. *Instability and Transition*, Vol 1, 426-439, Proceedings of ICASE/LaRC Workshop on Stability and Transition, Springer-Verlag, New York.

16. Panton, R. 1968. The transient for Stokes's oscillating plate: a solution in terms of tabulated functions. *J. Fluid Mech.* 31, 819-825.

17. Noble, B. 1958. *Methods Based on the Wiener-Hopf Technique*, Pergamon Press, London.

18. Van Dyke, M.D. 1964. Higher approximations in boundary layer theory. Part 3. Parabola in uniform stream. *J. Fluid Mech.* 19, 145-159.

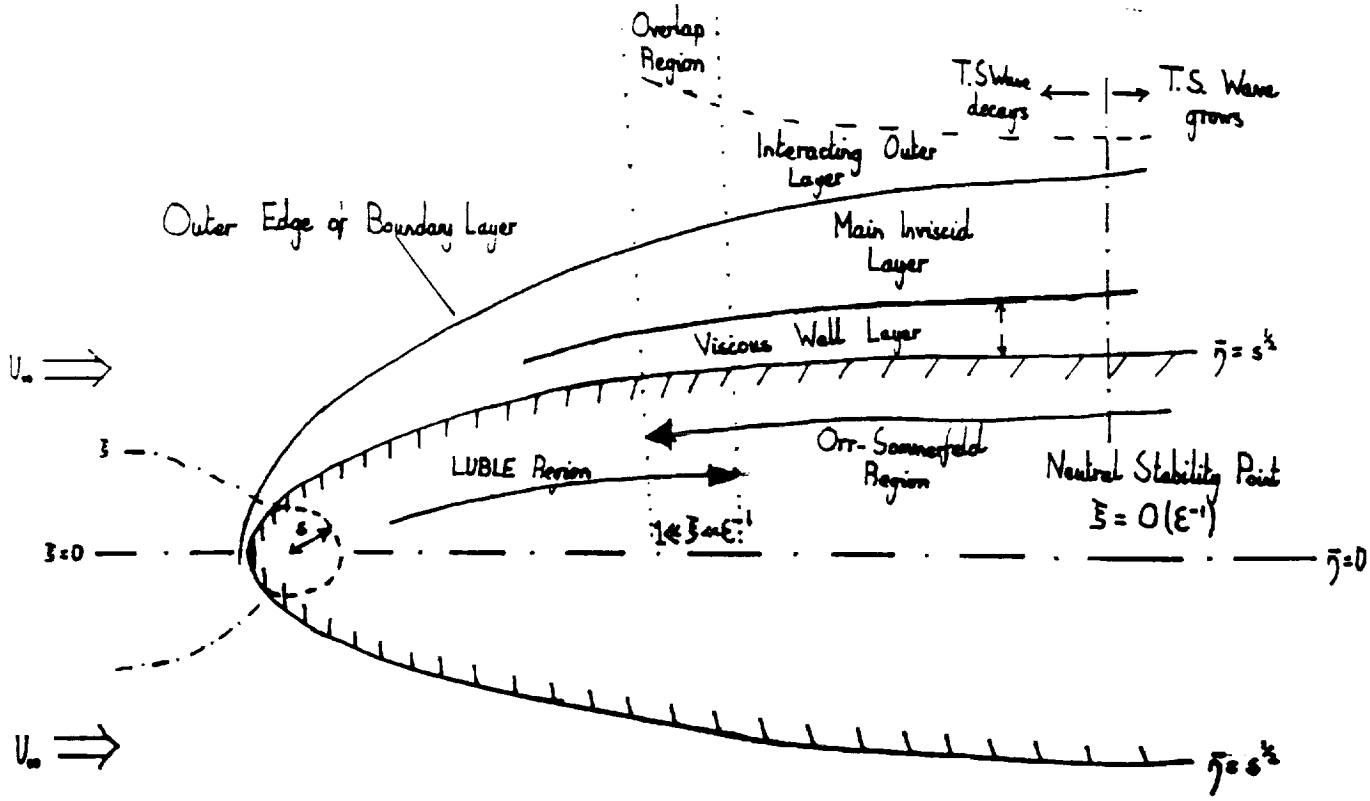

FIGURE 1. The asymptotic structure for the unsteady disturbances in the boundary layer of a parabolic cylinder.

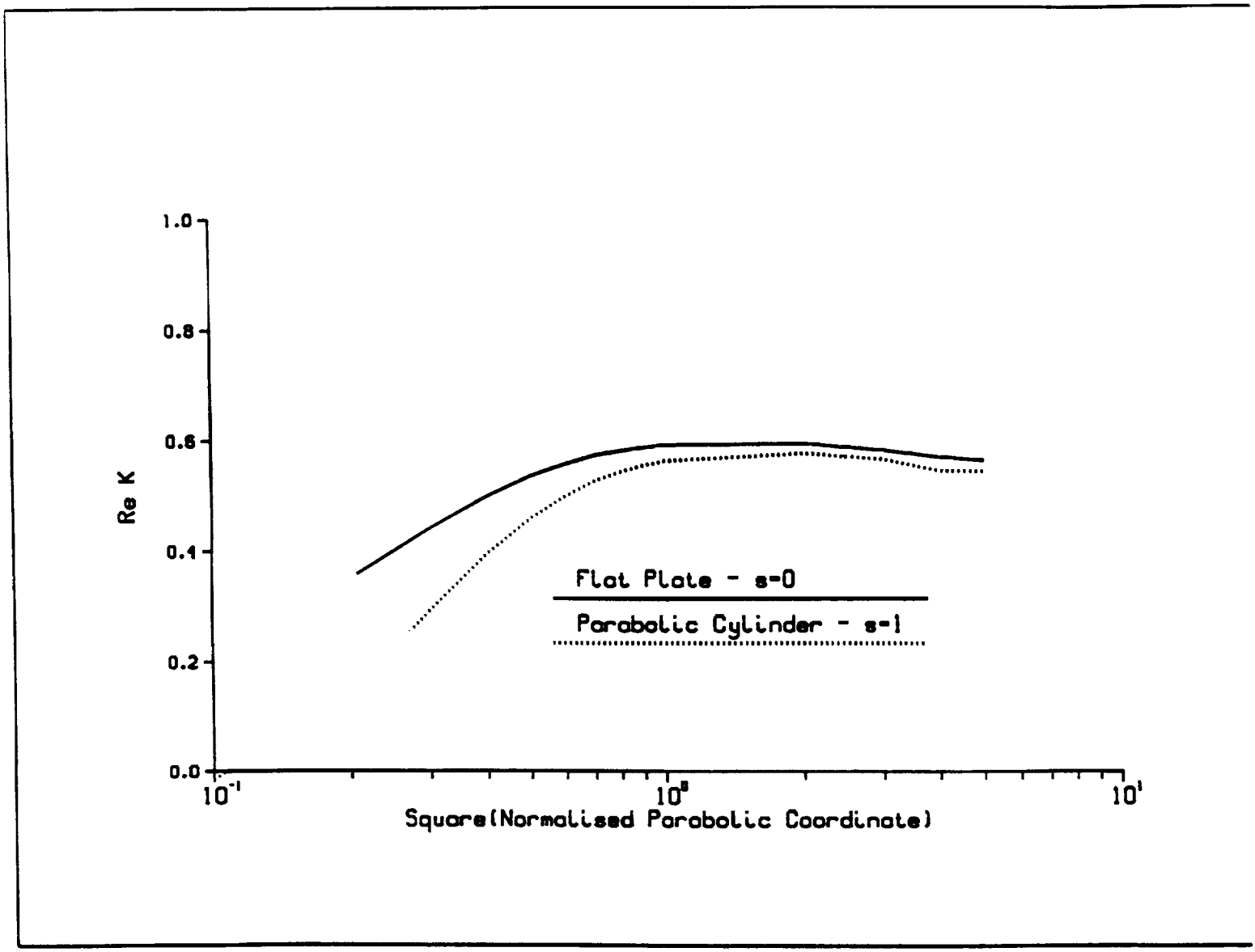

FIGURE 2. Variation of the real part of the TS wavenumber (multiplied by ϵ) as a function of the downstream distance ($\mathrm{Re}(\kappa)$ vs. $\tilde{\xi}_1^2 = (\xi_1/U_0')^2$) for $\epsilon \equiv (\omega\nu/{U_\infty}^2)^{-\frac{1}{6}} = 0.1$. The flat plate result is compared to that for a parabolic surface with $s \equiv \omega r_n/U_\infty = 1.0$, where r_n is the nose radius.

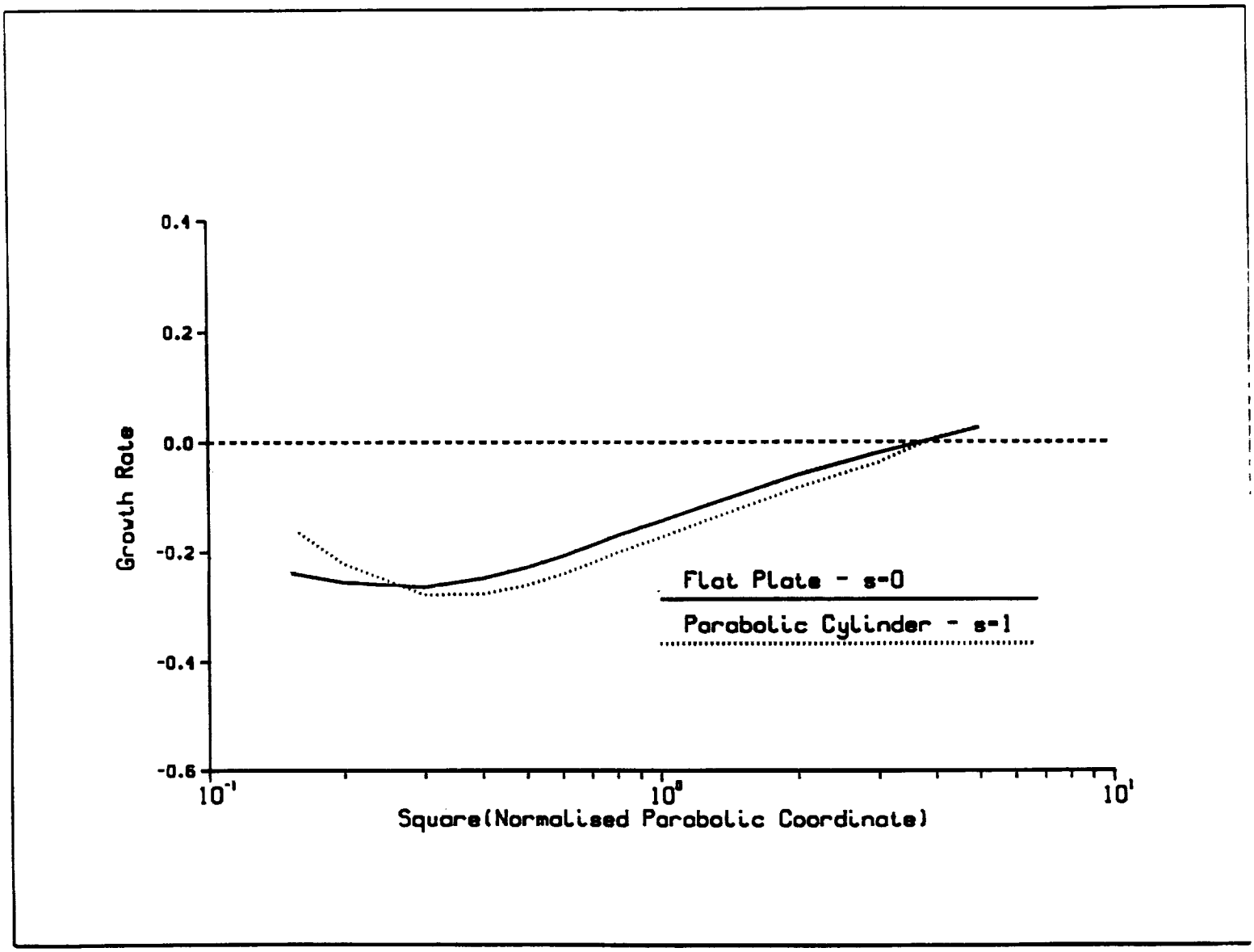

FIGURE 3. Variation of the growth rate of the TS wave (multiplied by ϵ) as a function of the downstream distance ($-\mathrm{Im}(\kappa)$ vs. $\tilde{\xi}_1^2 = (\xi_1/U_0')^2$). Flat plate results are compared with those for a parabolic cylinder with $s = 1$. The stabilising effect of the favourable pressure gradient can be seen, this effect decreasing with distance downstream as the body curvature approaches zero.